Characterization of a self-starting, passively mode-locked fiber ring laser that exploits nonlinear polarization evolution

V. J. Matsas, D. J. Richardson, T. P. Newson, and D. N. Payne

Optoelectronics Research Centre, Southampton University, Southampton S09 5NH, UK

Received September 21, 1992

A full characterization of a self-starting, passively mode-locked soliton ring fiber laser in terms of its various modes of mode-locked operation, cavity length, and type of fiber used is presented. Direct evidence, based on state-of-polarization measurements, that nonlinear polarization evolution is the responsible mode-locking mechanism is also given.

Passive mode locking of the erbium-doped fiber laser has recently attracted considerable interest, with schemes based on Sagnac interferometers[1] and fast saturable absorbers[2] so far demonstrated. Passive mode locking by using nonlinear polarization evolution (NLPE) as a self-sustaining mechanism has also been proposed and demonstrated in Fabry–Perot Nd^{3+} and Er^{3+} fiber lasers.[3,4] However, such systems were incapable of self-starting. Self-starting, passive mode locking of an Er^{3+} fiber ring laser has been briefly reported by Mollenauer[5] and investigated theoretically by Chen *et al.*[6] In a recent paper[7] we reported the self-starting, passively mode-locked operation of an all-fiber soliton ring laser incorporating an intracavity polarizer and a length of low-birefringence (Lo-Bi) fiber used as a nonlinear switch to exploit NLPE. In this Letter we describe the various regimes of operation of this system and characterize its behavior with respect to the cavity length and the type of the passive fiber used.

The experimental configuration, Fig. 1, is made of X m of passive fiber (X = variable), 3 m of Er^{3+}-doped fiber (dopant concentration = 800 parts in 10^6, N.A. = 0.15, λ_{co} = 960 nm, D = 13 ps nm^{-1} km^{-1}, estimated beat length $L_b = \lambda/\Delta n \sim 0.5$ m, where λ is the wavelength and Δn is the refractive-index difference between the slow and the fast axes), and a polarizing optical fiber isolator of unknown dispersion. Two types of passive fiber were used: a Lo-Bi spun fiber (N.A. = 0.1, λ_{co} = 1230 nm, D = 17 ps nm^{-1} km^{-1}, A_{mode} = 125 μm^2, and $L_b > 10$ m) and a standard telecommunications fiber (N.A. = 0.11, λ_{co} = 1200 nm, D = 17 ps nm^{-1} km^{-1}, A_{mode} = 100 μm^2, and $L_b \sim 2$ m). Two polarization controllers PC1 and PC2 were used to set the low-intensity (i.e., cw) state of polarization (SOP) entering and leaving the Lo-Bi fiber, respectively, which, because of the presence of the polarizer in the ring, controls the loss of the system in the linear regime. By using the PC's, the laser is encouraged to operate in pulsed mode by deliberately biasing the resonator to a high-loss state for cw (low-intensity) operation. Since the onset of NLPE alters the SOP of the light reaching the polarizer and thereby reduces the cavity loss, the laser will favor pulsed (high-intensity) operation. Pumping was provided by an actively stabilized Ti:sapphire laser operating at 980 nm.

Initially the laser was characterized using a 180-m length of Lo-Bi fiber and the SOP before the optical isolator was monitored as a function of pump power. The system's behavior was then further examined as a function of the length and the beat length of the passive fiber used.

Two distinct regimes of mode-locked operation were observed that depend on both the pump power and the polarization controller settings. The square-pulse regime was characterized by broad (30–40 nm) optical bandwidth, long-duration (>500 ps) square pulses at the cavity round-trip frequency, as also reported for the figure-eight laser.[2] This regime was observed for pump powers >150 mW. At lower pump powers (<150 mW) the only pulsed mode-locked operation obtained was solitonic.

This second regime was characterized by soliton pulses randomly spaced in the time domain, with the pulse patterns repeating at the cavity round-trip frequency. Average repetition rates as high as 10 GHz were observed. The PC's setting affected both the pulse width and, to a lesser degree, the operating wavelength. Figure 2 shows the evolution in the optical spectrum of the laser as the pump power is raised. The onset of mode-locked operation is marked by an abrupt change in the spectrum at a particular value of the pump power. The narrow cw line

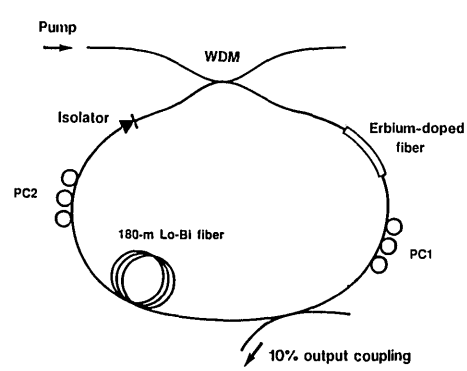

Fig. 1. Experimental setup. WDM, wavelength-division-multiplexing coupler.

0146-9592/93/050358-03$5.00/0

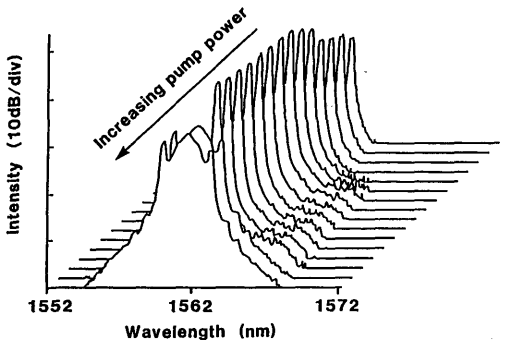

Fig. 2. Optical spectrum variation with increasing pump power showing onset of mode locking.

develops into a much broader, approximately sech^2 spectrum that possesses two distinct, symmetrically located side lobes.[8] The onset of mode locking was often accompanied by an additional cw component (an additional sharp spectral feature on the soliton spectrum) that could subsequently be eliminated on reduction of the pump power.[9] Once mode locking had been initiated, decreasing the pump power produced discrete and abrupt jumps (downward) in the laser output power, coinciding with the disappearance of individual pulses from the cavity. This process would continue until only one pulse would remain inside the laser cavity (fundamental mode locking). Autocorrelation measurements showed that, for the 180-m cavity, by tuning the PC's the pulse width could be varied between 1.55 ps and approximately 4 ps, with corresponding ratios of soliton period to total cavity length of 0.29 and 2, respectively. The autocorrelation traces were found to be well fitted by sech^2 pulse forms and were pedestal free (e.g., see Ref. 7). It should be noted that sidelobe suppression improved as the pulse duration was increased (or equivalently as the ratio of the cavity length to soliton period decreased), as expected from the theory based on the average soliton approach presented in Ref. 8. By appropriate PC control, the sidelobe intensity was effectively suppressed >40 dB relative to the central peak for the longest-duration pulses. The pulse duration also depended on the pump power. When operating with the PC's set to give minimum pulse duration, the pulse width narrowed from 2 ps at a pump power of 150 mW down to 1.55 ps at a power of 30 mW. The time–bandwidth products at these pump powers were 0.38 and 0.32, respectively. The wavelength tuning range was of the order of 5 nm, although mode-locked operation could be obtained around both 1.538 and 1.558 μm. In addition, simultaneous mode-locked operation at as many as three central frequencies was also observed during the course of these experiments.

In the soliton regime two further distinct operating modes were observed, depending on the setting of the PC's. The difference between the two is most strikingly demonstrated by observing their spectral behavior as a function of pump power [compare Figs. 3(a) and 3(b)]. In mode #1 [Fig. 3(a)], the central wavelength and spectral shape of the pulses remained constant as the pump power was varied. The ratio of the amplitude of the sidelobes to that of the central frequency was generally found to depend on the pump power (as well as depending on the PC's setting as mentioned above). This mode exhibits the hysteresis and the discrete jumps observed in the output power characteristic owing to energy quantization of the pulses as first observed in the figure-eight laser.[9] By measuring the size of the power jumps on the disappearance of individual pulses from the cavity, the energies of the individual pulses intracavity have been found to be close to those expected for fundamental solitons.[7] Immediately after a jump in pulse number, any excess energy above that required to support the reduced number of pulses is removed by energy shedding into the dispersive wave and absorption at the nonlinear switch. The appearance of any pedestal component in the autocorrelation trace as a result of this process was not observed, although slight changes in pulse

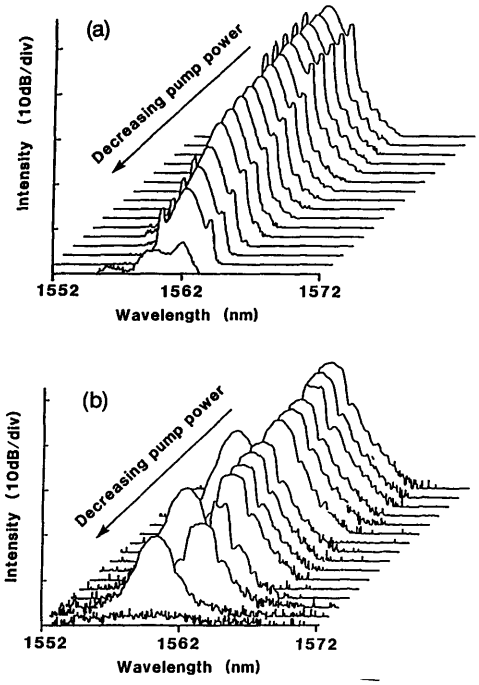

Fig. 3. Optical spectrum variation for (a) operating mode #1 and (b) operating mode #2 with decreasing pump power. The y axis is logarithmic with arbitrary power units, and the resolution is 0.1 nm.

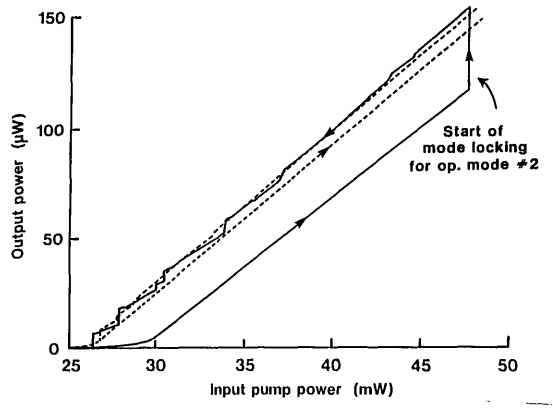

Fig. 4. Power hysteresis curves for operating modes #1 (dashed curves) and #2 (solid curves).

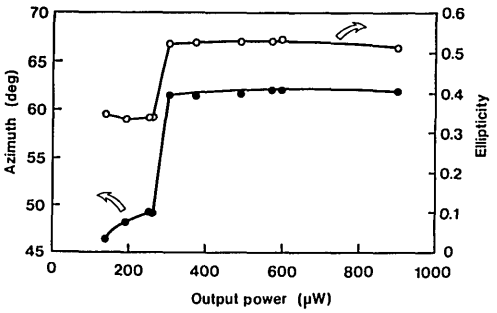

Fig. 5. Ellipticity and azimuth of the light emerging from the output port located before the isolator as a function of pump power.

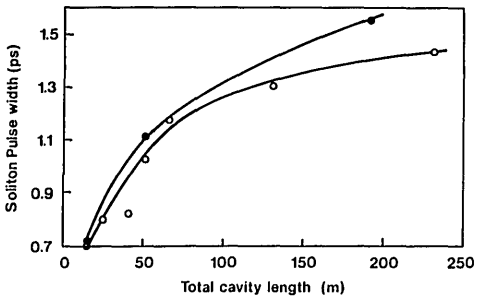

Fig. 6. Minimum soliton pulse width versus total cavity length for the two types of fiber used.

width when a small number of pulses were present in the cavity were observed.

In mode #2 [Fig. 3(b)], discrete changes in the central wavelength and spectral shape were observed with varying pump power. These became particularly prominent at pump powers close to the cw threshold value. The output power characteristic of the laser for the two soliton modes is shown in Fig. 4. In mode #1 (dashed curves) the cw threshold was found to be 27 mW. Mode locking was found to self-start at a second threshold of 70 mW (not shown). A higher cw threshold of 30 mW was observed for the system operating in mode #2 (solid curves, Fig. 4); however, the second threshold was now reduced to 47 mW. Once initiated, mode locking could be maintained at pump powers significantly lower than the cw threshold. Abrupt jumps, both upward and downward, in the output power were observed in this instance. Downward jumps were associated with pulse disappearances and were not constant from jump to jump, particularly when a small number of pulses remained in the cavity. The much smaller upward jumps were associated with discrete wavelength shifts (~3 nm). The fundamental difference between these two soliton modes is currently not understood.

An extra 90:10 coupler was placed immediately before the polarizing optical isolator, and the SOP of light emerging from the output port of this coupler was monitored as a function of pump power by using a real-time polarization analyzer (Electro-Optic Development). Unfortunately, this instrument employs a fiber input lead of unknown birefringence, and therefore a measurement of the absolute state of polarization at the polarizer input was not possible. The device could, however, be used to detect changes in the polarization state. The results of the measurements are shown in Fig. 5. It was observed that the SOP at the output port remained approximately constant during cw operation up until the onset of mode locking, at which point an abrupt change in the SOP was observed. The SOP remained fixed at pump powers beyond this point. This observation provides strong evidence that NLPE provides the mode-locking mechanism within this laser.

The Lo-Bi fiber section was cut back to a length of 45 m and subsequently to 3 m in order to measure the minimum pulse width obtainable as a function of the total cavity length. The length of the residual fiber in the cavity (i.e., erbium-doped fiber amplifier, isolator pigtails, and coupler leads) was ~15 m. The shortest pulses obtained had a duration of 720 fs with the 3-m Lo-Bi fiber section. Similar measurements were made with a section of standard telecommunications fiber. Lengths of fiber ranging from 200 down to 3 m were tested. The shortest pulse observed with this fiber was 700 fs. Figure 6 summarizes the pulse-width dependence on the total cavity length for the two types of fiber used. It is seen that the pulse width follows an approximate $L^{1/2}$ dependency in both cases. With a maximum pump power of 100 mW, no spontaneous mode locking was observed without at least a 3-m section of relatively Lo-Bi ($L_b > 2$ m) fiber within the fiber laser cavity. When sections of medium to highly birefringent fiber ($L_b < 0.1$ m) were incorporated within the cavity, no mode locking was observed, irrespective of the fiber length used. Finally, in terms of ability to self-start and in terms of spectral quality and overall stability, the Lo-Bi fiber produced significantly better results than the ordinary telecommunications fiber.

V. J. Matsas thanks the Committee of Advanced Studies of Southampton for the provision of a studentship. This study was partly funded by the European Economic Community Race project R2015 (ARTEMIS).

References

1. I. Duling III, Electron. Lett. **27,** 544 (1991); D. J. Richardson, R. I. Laming, D. N. Payne, V. J. Matsas, and M. W. Phillips, Electron. Lett. **27,** 730 (1991).
2. M. Zirngibl, L. W. Stulz, J. Stone, J. Hugi, D. Digiovanni, and P. B. Hansen, Electron. Lett. **27,** 1734 (1991).
3. M. Hofer, M. E. Fermann, F. Haberl, M. H. Ober, and A. J. Schmidt, Opt. Lett. **16,** 502 (1991).
4. R. P. Davey, N. Langford, and A. I. Ferguson, Electron. Lett. **27,** 1257 (1991).
5. L. Mollenauer, in *Digest of Conference on Optical Fiber Communication* (Optical Society of America, Washington, D.C., 1991), p. 200.
6. C. J. Chen, P. K. A. Wai, and C. R. Menyuk, Opt. Lett. **17,** 417 (1992).
7. V. J. Matsas, T. P. Newson, D. J. Richardson, and D. N. Payne, Electron. Lett. **28,** 1391 (1992).
8. S. M. J. Kelly, Electron. Lett. **28,** 806 (1992).
9. A. B. Grudinin, D. J. Richardson, and D. N. Payne, Electron. Lett. **28,** 67 (1992).